Long-term hybridization in a karst window reveals the genetic basis of eye loss in cavefish

Riley Kellermeyer[1,2*], Chris Seidel[1], William B. Redwine[1], Rachel L. Moran[3], Sylvain Bertho[1], Claudia Patricia Ornelas-García[4], Dana Alegre[1], Kyle Weaver[1], Jay Unruh[1], Benjamin Troutwine[1], Yongfu Wang[1], Emily Collins[5], Jennifer Rutkowski[1,5], Suzanne E. McGaugh[2], Luis Espinasa[5] and Nicolas Rohner[1*]

[1] Stowers Institute for Medical Research, Kansas City, MO, USA
[2] Department of Ecology, Evolution, and Behavior, University of Minnesota, Minneapolis, MN, USA
[3] Department of Biology, Texas A&M University, College Station, TX, USA
[4] Colección Nacional de Peces, Departamento de Zoología, Instituto de Biología, Universidad Nacional Autónoma de México. Tercer Circuito Exterior S/N. CP 04510, Mexico City. México
[5] School of Science, Marist College, Poughkeepsie, NY, USA

* Corresponding authors

Abstract

Eye loss is a hallmark trait of animals inhabiting perpetual darkness, such as caves. The Mexican tetra (*Astyanax mexicanus)* provides an unparalleled model for studying the genetic basis of eye loss. There are two interfertile morphs of the Mexican tetra, sighted surface fish and multiple independently evolved eyeless, blind cavefish populations. Despite decades of research on eye loss in this species, our understanding of the precise genetic basis remains sparse. Here, we focused on the unique Caballo Moro cave, where there is a karst window collapse that introduced sunlight and coexistence of both eyed and eyeless cavefish of similar genetic background. This unique genetic mosaic allowed us to pinpoint coding mutations in Connexin 50 (Cx50), also known as gap junction protein alpha 8b (Gja8b), as critical in the genetic basis of eye loss. CRISPR based knockouts of Cx50 in surface fish result in small or absent eyes as young as 48 hours post-fertilization. Further, we identified similar mutations in Cx50 that alter predicted protein structure among other cave-dwelling fish and even subterranean mammals, indicating a conserved evolutionary mechanism of Cx50 mutations. We introduced a mutation (Cx50-S89K) in mice, which resulted in cataracts, smaller eyes, and smaller lenses. Mutations in Cx50 mimic those identified in human congenital cataracts. We additionally leveraged phenotypic variation in a hybrid cavefish population to demonstrate that eyes provide fish with a metabolic advantage, providing a mechanism by which loss of eyes could be favored by selection. This unique hybridization event allowed us to identify novel alleles that contribute to the convergent evolution of eye loss, providing profound insights into the genetic underpinnings of one of nature's most fascinating adaptive traits.

Introduction:

Cave-dwelling and subterranean organisms across a diverse range of taxa exhibit morphological and physiological adaptations tailored to the unique challenges of their underground habitats. Among these adaptations, the loss or reduction of eyes is one of the most conspicuous and consistent traits in subterranean animals. Loss of eyes is hypothesized to be driven by the metabolic cost of eyes and futility of vision in total darkness (Aiello & Wheeler, 1995; Hüppop, 1986; Lacey, 2000; Moran et al., 2015). The recurrent pattern of eye degeneration across various species can be leveraged to provide valuable insights into the mechanisms and constraints of repeated evolution.

Despite decades of work on a variety of species, surprisingly little is known about the precise genetic basis responsible for eye loss in any subterranean animal. Most work has been performed on *Astyanax mexicanus*, a remarkable model for cave adaptations. *Astyanax mexicanus* has two morphs- eyeless cavefish and eyed surface fish. The surface fish represent the ancestral state of the derived cave morph, and the two morphs remain interfertile. Cave-morphs have independently evolved multiple times in the Sierra de Guatemala and Sierra de El Abra regions of Mexico (Espinasa, 2018; Gross, 2012; Moran et al., 2023; Policarpo et al., 2024). There are currently 35 known *Astyanax* cave populations that are eyeless or have severely reduced their eyes (Espinasa et al., 2018, 2020; Miranda-Gamboa et al., 2023; Mitchell et al., 1977). As such, eye loss in *A. mexicanus* cavefish offers a natural experiment of repeated evolution.

Quantitative Trait Loci (QTL) analyses have linked eye size with genotypes in lab-reared, cave x surface F2 hybrids, identifying over 14 genomic regions that influence eye size (Borowsky & Wilkens, 2002; McGaugh et al., 2014; O'Quin et al., 2013; Protas et al., 2007; Warren et al., 2021; Wiese et al., 2024). However, the resolution of QTL studies is limited by the number of recombination events and sample sizes, resulting in thousands of potential variants within these broad, eye-associated genomic intervals. Beyond QTL mapping, key developmental regulators such as *pax6* and *shh*, along with epigenetic factors, have been implicated in eye loss (Gore et al., 2018; Jeffery & Martasian, 1998; Yamamoto et al., 2004). Despite decades of research into the genetic basis of eye loss in this species, to our knowledge not a single protein coding mutation has been identified as contributing to eye loss. The only functionally-validated genetic factors underlying this trait are reduced expression of *rx3* and a *cis*-regulating hypomorphic mutation that disrupts optic vasculature (Ma et al., 2020; Warren et al., 2021).

Here we took advantage of a natural experiment in the Caballo Moro cave to identify novel genes involved in eye degeneration. Located within the Sierra de Guatemala cave system (Figure 1a), the Caballo Moro cave is the result of a relatively recent, partial cave ceiling collapse (Mitchell et al., 1977). The resulting karst window introduced part of an 80 m long cave lake to sunlight, a rarity for caves that typically exist in perpetual darkness (Figure 1b, Extended Data Fig. 1). Lit areas of the lake are now inhabited by fish with similar morphology to surface fish, including fully developed and functional eyes (Figure 1c, d). Blind, eyeless cavefish inhabit the dark side of the lake (Figure 1e; Espinasa & Borowsky, 2000). This unique cave provides a rare scenario where dimorphic eyed and blind cavefish coexist in the same pool with no geographic barriers.

Despite the opportunity for gene flow, fish in Caballo Moro are either fully eyed or completely eyeless, with only two fish observed with an intermediate eye phenotype out

of 75 surveyed fish between this and a previous study (Espinasa & Borowsky, 2000). The striking dichotomy in eye morphology within fish in the Caballo Moro cave suggests that selective pressures favor the retention of these distinct traits, despite individuals being interfertile and in proximity. Previous RAPD analysis of eyed and eyeless Caballo Moro cavefish showed that both morphs in this cave are closely related to other cavefish in the region, eliminating the possibility that the eyed fish are recent surface immigrants (Espinasa & Borowsky, 2000). Currently, two hypotheses exist for the origin of the eyed fish: 1) they could be descendants of cave-surface hybrids or, less likely, 2) they represent an evolutionary reversion to an ancestral eyed state (Dollo's Law; Dollo, 1893, 1922; Niemiller et al., 2013). Either scenario, however, would allow finer-scale genetic mapping of eye loss compared to QTL studies.

Through whole genome sequencing of eyed and eyeless Caballo Moro fish, we found that the eyed cavefish stem from a cave-surface hybridization event that occurred ~15,000 generations ago. Ongoing hybridization allowed us to identify relatively few SNPs differentiating the eyed and non-eyed fish, suggesting these SNPs may be related to eye loss. Using genome-wide association and genotype filtering, we identified a coding mutation in a phylogenetically conserved region of the lens *connexin-50* (*cx50*; also known as *gap junction protein alpha 8b* or lens membrane protein 70) linked to smaller eye sizes and cataracts. Knocking down *cx50* in surface fish resulted in absent or small eyes. We linked mutations in *cx50* to body condition in a wild, hybrid population. Notably, we identify other variants in highly conserved regions of *connexin-50* across independently derived *Astyanax* cavefish and other species of subterranean fish and mammals. Protein modeling of these subterranean variants and functional validation of a variant in a mouse model places *cx50* as a potential example of gene reuse in convergent eye degeneration phenotypes.

Results:

Eyed Caballo Moro cavefish are longstanding cave-surface hybrids

To determine the origin of the eyed fish from the Caballo Moro (CM) cave, we collected 19 light-dwelling eyed fish and 17 dark-dwelling eyeless fish from the cave, and six surface fish from nearby surface environments (Fig. 1a). Anatomical and behavioral characterizations revealed that the eyed Caballo Moro cavefish, despite having eyes, exhibit other phenotypes that are typically associated with cavefish, including Vibration Attraction Behavior (VAB), fused suborbital bones, a smaller optic tectum, extra maxillary teeth, and large eggs (Extended Data Fig. 2, 3a-b; Atukorala & Franz-Odendaal, 2018; Espinasa et al., 2021; Hüppop & Wilkens, 1991; Soares et al., 2004; Yoshizawa et al., 2010). In two visits 20 years apart, eyed fish were observed to chase eyeless fish from the illuminated side of the pool (Espinasa & Borowsky, 2000). This observation led us to investigate whether behavior contributes to the spatial segregation of the eyed and blind cavefish within the same cave environment. In a controlled resident-intruder assay, we exposed eyed CM fish to both surface and eyeless intruders, separated by a glass pane, and counted the number of strikes taken at intruder fish (Extended Data Fig. 3c-d; Elipot et al., 2013). Eyed CM fish attack both eyeless CM fish and surface fish, while surface fish preferentially attack other surface fish ($p<0.0001$, Kruskal-Wallis test). These behavioral findings not only confirm that the eyed CM fish have functional vision but also

suggest aggression as a potential source of the geographical separation of the different morphs within the cave.

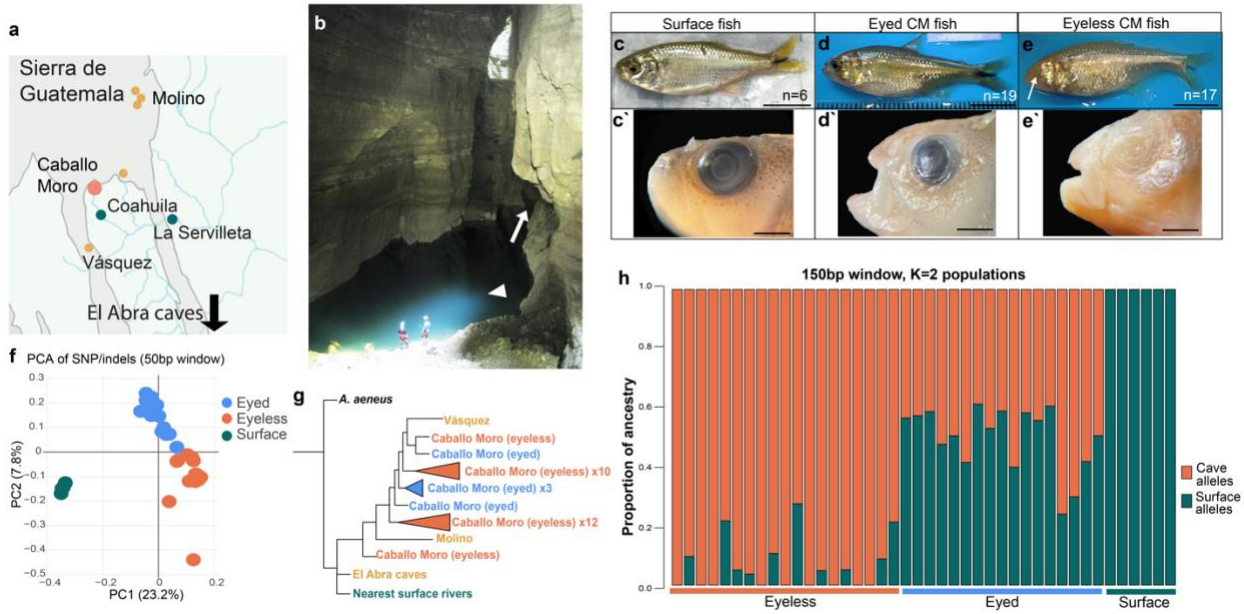

Figure 1. Caballo Moro cavefish and their ancestry. (a) Map of the Sierra de Guatemala area caves. Location of Caballo Moro (large orange dot) and other caves (small orange dots) in the Guatemala region. Nearby surface fish were sampled from Coahuila and La Servilleta rivers for comparison (green). Arrow indicates that the El Abra caves are further south of the figure. **(b)** The Caballo Moro cave pool. Collapse of the roof of the cave exposed part of the cave pool to sunlight (arrowhead) while most of the cave remains in darkness (arrow). **(c-e')** Examples of fish sampled and sequenced. Whole fish scale is 10mm, eye closeup is 2mm. **(c,c')** Fish collected from nearby surface rivers. **(d,d')** Eyed Caballo Moro cavefish collected from the light side of the cave. **(e,e')** Eyeless Caballo Moro cavefish collected from the dark side of the cave. **(f)** Principal component analysis of SNPs and indels compared to the surface reference genome. **(g)** Consolidated phylogeny of the Caballo Moro cavefish in relation to nearby caves and surface rivers sampled from (Moran et al., 2023). **(h)** Admixture analysis of 679,525 biallelic, statistically unlinked sites. Sites from each individual are sorted into ancestral populations (K=2) with 150bp windows and plotted as admixture coefficients.

To unravel the population structure and ancestry of the Caballo Moro cavefish, we sequenced all 36 cave individuals and the six surface fish to an average coverage depth of 8.7X and conducted population structure and admixture analysis (Extended Data Fig. 4a; see Methods). In a principal component analysis (PCA) of SNPs and indels, the eyed and eyeless CM fish clustered as closely related but distinct subpopulations. The eyed and eyeless subpopulations clustered separately from surface fish, with eyed fish slightly closer to surface than eyeless (Fig. 1f, Extended Data Fig. 4b). This population structure is further supported by genome-wide nucleotide diversity calculated in each subpopulation (Supplementary Information 1). The genome-wide nucleotide diversity (π)

was nearly ~1.5 times higher in the surface population (π = 0.00772) compared to the eyeless population (π = 0.00461). Nucleotide diversity for the eyed ecotype was intermediate between the eyeless and surface populations (π = 0.00567). Next, we evaluated a paired down phylogeny produced by Moran et al. (2023) with individuals from the CM cave and 26 additional populations. The resolved phylogeny for the Caballo Moro cavefish showed that both the eyed and eyeless fish cluster with Vásquez and Molino, two geographically close Guatemala cave populations, and are diverged from surface populations (Fig. 1g, Extended Data Fig. 4c). These patterns suggest that the eyed cavefish are cave-surface hybrids.

To further investigate the ancestry of the eyed cavefish, we conducted admixture analysis with a range of potential ancestral populations (K=1-5). We found that this dataset is best modeled by the surface fish and eyeless cavefish accounting for the two parental populations, and the eyed cavefish as an admixed population resulting from hybridization between cave and surface fish (Fig. 1h, Extended Data Fig. 5). Following Moran et al. (2021), we used eyeless fish and surface fish as parental population to estimate the number of generations since the putative hybridization event with a hidden Markov model (HMM). Using this model, we found that eyed CM individuals carry ~12% surface ancestry, which is in line with an early hybridization event followed by selection on genotypes that provide advantages in the lighted area of the caves. The mean ± SE genome-wide proportion of ancestry derived from the cave parental population was 0.89 ± 0.066. The mean ± SE tract length from the surface parental population was 7,710 ± 919 bp. Based on these findings, we estimate that there have been 15,740 generations since the initial cave-surface hybridization event. While there are limitations in estimating the number of generations, if we assume a single generation per year, this would put the onset of hybridization in line with geological observations that the cave collapsed less than 20,000 years ago, as there is still large, visible debris from the collapse (Extended Data Fig. 1d; Zhao & Shen, 2022). This rough estimate suggests that the timing of the hybridization is consistent with an end of Pleistocene to Holocene event, near the end of the ice age or afterwards.

These combined data strongly suggest that eyed CM fish are the result of long-standing cave-surface hybridization, the equivalent of a long back-crossing experiment. Approximately 15,000 generations of recombination have broken up the surface and cave regions on the chromosome while maintaining distinct eye phenotypes. We can therefore use this unique dimorphic cave population to conduct fine mapping of the genetic origins of the eye loss phenotype.

Candidate genes for eye degeneration

We took a multi-tiered approach to identify genes associated with the eyeless versus eyed phenotype. We conducted a genome-wide association study (GWAS) to find chromosomal regions linked to the eye phenotype. In a Cochran-Armitage trend test with SNPs and indels in eyeless CM fish compared to both eyed and surface fish, we identified 7 chromosome regions, encompassing 438 genes (Cochran-Armitage trend test filtered to -log10(p)>10; Fig. 2a, Supplementary Information 2).

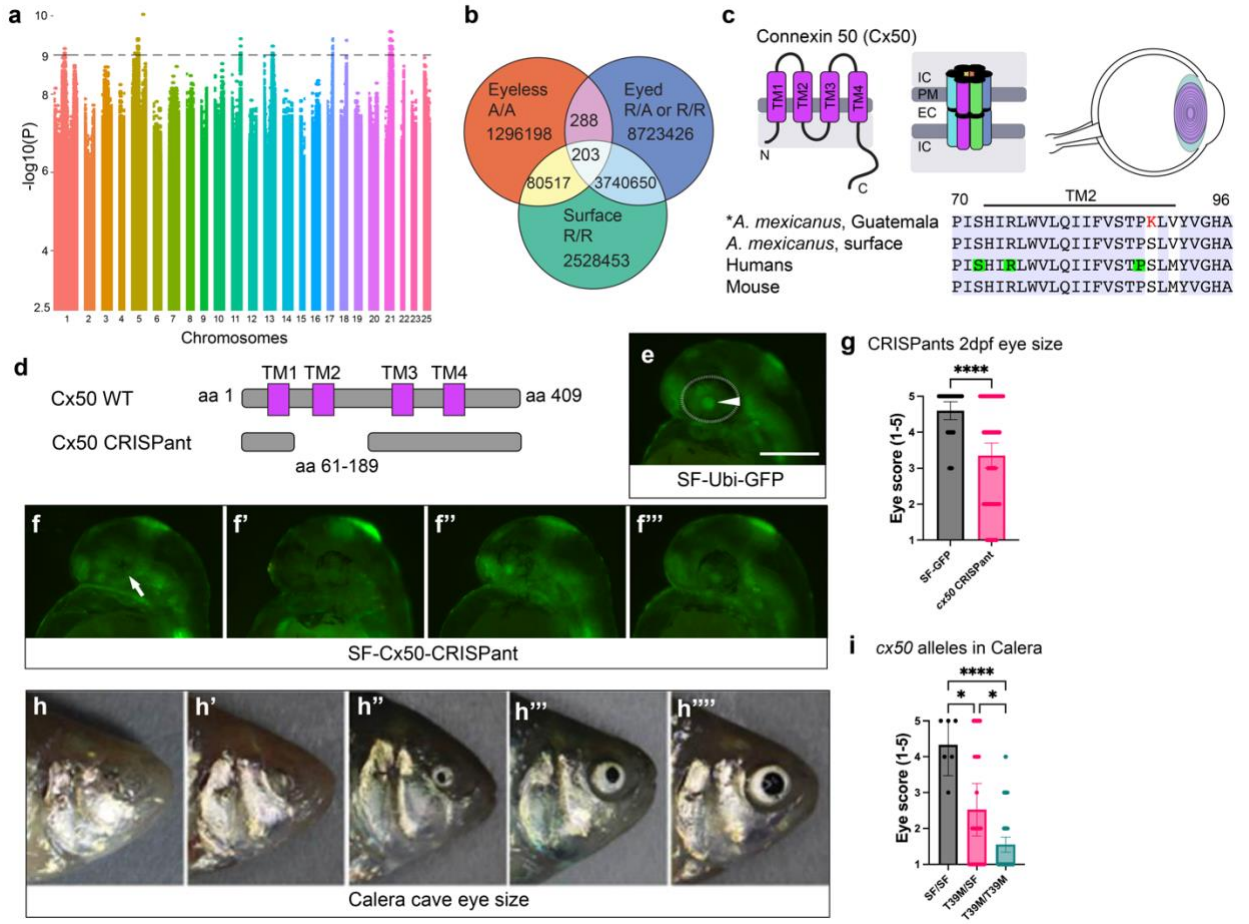

Figure 2. Candidate gene selection and Cx50 CRISPants. (a) Manhattan plot of a Cochran-Armitage trend test GWAS comparison of eyeless SNPs to both eyed and surface SNPs. Horizontal line indicates -log10(p)>9. Seven locations associated with eye loss were identified encompassing 7,373 SNPs and 438 genes. **(b)** Intersect of SNPs in surface, eyed, and eyeless fish. Surface fish were sorted for having surface-reference only alleles (Reference/Reference). Eyed fish were filtered to SNPs with at least one reference allele (R/R or Reference/Alternate). Eyeless fish were filtered to homozygous for an alternate allele (Alternate/Alternate) compared to the surface reference. 203 SNPs were found that meet these criteria, falling within 41 annotated genes and *cis*-regulatory regions. **(c)** Diagram of Cx50 and comparison of protein sequence in Guatemala-region caves (including Caballo Moro), surface fish, humans, and mice. Gap junctions are formed by six gap-junction proteins, each with 4 transmembrane domains. Cx50 is expressed primarily in the lens (purple) to connect cells for lens fluidity. Green highlights indicate sites of known human CX50 SNPs that contribute to congenital cataracts or small eyes. Red text indicates the site modified in eyeless cavefish when compared against eyed CM and surface fish **(d)** Schematic of Cx50 TM2 region targeted in CRISPants. CRISPants were defined as more than 99% of sequenced reads with the deletion. **(e-f)** 2dpf surface fish with transgenic ubiquitin-GFP (SF-Ubi-GFP; Stahl et al., 2019) expression from the same clutch. Ubi-GFP allows visualization of the lens (arrowhead). Bar is 500µm. **(e)** Un-injected SF-Ubi-GFP with wild-type eye size, a score of 5 (n=15 fish; both eyes scored, n=30). Arrowhead

indicates the lens; outline is the eye. **(f-f''')** The spectrum of eye phenotypes in Cx50 CRISPants ranked by increasing eye size, representing eye size scores from 1 through 4 from left to right (n=37 fish; both eyes scored, n=74). Note the complete collapse of eye and pigment cells into a single point in score 1 (arrow), and the absence of a lens in score 2. A lens is generally visualized in scores above 3. **(g)** Quantification of eye size score between uninjected transgenic fish and CRISPants ($p<0.0001$, two-tailed Mann-Whitney U test, error bars are 95% confidence interval). **(h-h'''')** Sample of eye sizes from the hybrid population in the Calera cave, with scores of 1-5 (n=121 fish, both eyes scored, n=242). **(i)** Quantification of eye scores in Calera cavefish by Cx50-T39M genotypes. Surface fish allele (SF) homozygous (SF/SF) versus heterozygous (T39M/SF) $p=0.0012$; T39M/SF versus homozygous cave allele (T39M/T39M) $p=0.0013$; Surface homozygous versus cave homozygous (T39M/T39M) **** $p<0.0001$; Kruskal-Wallis test with Dunn's multiple comparison, error bars are 95% confidence interval.

To further refine our candidate gene selection, focusing particularly on those most likely contributing to the eyeless phenotype, we filtered for SNPs that were homozygous for the alternate allele in all eyeless samples relative to the surface reference. We intersected the SNPs with reference alleles present in both the eyed fish and surface fish. The result was 203 SNPs, in 41 annotated genes (Fig. 2b, Supplementary Information 3), of which 199/203 (98%) were found in non-coding regions of the genome, in line with previous estimates that a large share of genetic changes are in regulatory regions (Gore et al., 2018; Krishnan & Rohner, 2017). Notably, 24 of these genes and those determined via GWAS overlap with regions previously identified in quantitative trait loci (QTL) studies for eye phenotypes and known zebrafish eye genes (Supplementary Information 4; Wiese et al., 2024).

From these 24 candidate genes, *connexin-50* (*cx50*) has a nonsynonymous serine to lysine (S89K) substitution and stood out for several reasons. First, the closest human homolog to Cx50, CX50 (or GJA8) is a lens-specific gap-junction protein that is essential for development, homeostasis, and transparency of the lens. Second, the S89K mutation in *cx50* affects a highly conserved amino acid within an important transmembrane domain. Additionally, *cx50* is located within a region undergoing a hard selective sweep in cavefish populations, indicative that *cx50* is under strong positive selection in cavefish (Moran et al., 2023). This mutation has also been mapped to previously identified eye-associated QTLs, reinforcing its potential importance in the evolution of the eyeless phenotype in cavefish (Lyon et al., 2017; Protas et al., 2007, 2008).

Connexin-50 and eye degeneration in *A. mexicanus*

In *A. mexicanus*, the lens acts as a master regulator of eye regression, as demonstrated by reciprocal lens transplantations between cave and surface fish (Yamamoto & Jeffery, 2000). Both morphotypes exhibit similar eye development until ~ 24 hours post fertilization (hpf), after which the cavefish lens undergoes a massive apoptotic event that causes the eye to completely degenerate (Alunni et al., 2007; Jeffery & Martasian, 1998).

CX50 is primarily expressed in the lens and forms an intercellular channel between adjacent cells comprising of 12 connexin units (Fig. 2c; Myers et al., 2018; Ping et al., 2021). CX50 is the only connexin present in interior lens fibers and is essential for maintaining homeostasis and fluidity in the lens (Berthoud & Ngezahayo, 2017; White et al., 1998). In humans, more than 40 SNPs in *CX50* have been identified that disrupt gap junction function, resulting in congenital cataracts and microphthalmia (small eyes), as the result of reduced lens fiber differentiation and increased apoptosis (Li et al., 2019; Minogue et al., 2009). Notably four of these disease-causing SNPs in humans occur just one amino acid upstream of the S89K mutation we found in eyeless Caballo Moro fish (Arora et al., 2006; Berry et al., 2020; Ge et al., 2014; Jin et al., 2022; Pal et al., 1999; Shiels et al., 1998; Vanita et al., 2008).

Cx50 is expressed in the lens in surface *A. mexicanus* at the key developmental timepoints and is downregulated in cavefish at 24 hpf and 54 hpf (Biswas et al., unpublished; Gore et al., 2018; Wiese et al., 2024). To confirm the role of Cx50 in *A. mexicanus* eye development, we generated surface fish F_0 CRISPants using *cx50*-targeted CRISPR guides (Fig. 2d-f; Stahl et al., 2019). *Cx50* knockouts showed small or no eyes at 2 days post-fertilization (dpf; $p<0.0001$, Mann-Whitney U test). Additionally, ~5% of *cx50* CRISPants at 2dpf displayed a cyclops phenotype (Supplementary Information 5). Together these results show that Cx50 is necessary for normal eye development in surface fish.

Astyanax mexicanus cavefish evolved through at least two independent events from ancestral surface fish populations colonizing caves in the Sierra de Guatemala and the Sierra de El Abra regions (Bradic et al., 2012; Garduño-Sánchez et al., 2023; Gross, 2012; Moran et al., 2023). Given the close relationship of Caballo Moro cavefish to other populations in the Guatemala region, we sequenced *cx50* in other Guatemala populations, including Molino, Escondido, and Jineo and found that they all share the S89K allele. We next asked if the same mutation is present in El Abra lineage fish. We sequenced individuals from the Pachón, Los Sabinos, Tinaja, Curva, and Calera populations and found that these cavefish carry the wildtype sequence at the S89 position. However, we found that all these populations carry an alternate mutation further upstream in the gene: a threonine to methionine (T39M) substitution. Notably, this highly conserved site in the first transmembrane domain of CX50 corresponds to the location of a known human SNP associated with cataracts (T39R; Ceroni et al., 2019; Sun et al., 2011; Tong et al., 2021). To explore the effects of this mutation, we generated F2 hybrids by crossing surface fish with Tinaja cavefish from the El Abra lineage. We genotyped 78 F2 hybrids for *cx50* and measured eye size. We found a correlation between reduced eye size and the presence of the Cx50-T39R variant (Extended Data Fig. 6a, $p=0.0163$, Kruskal-Wallis test).

To explore the effects of this mutation in the wild, under natural environmental conditions, we conducted field studies in the Calera cave, which has an independent evolutionary origin of the cave morph from Caballo Moro. Fish from the Calera cave show a large amount of surface gene flow, resulting in a spectrum of eye sizes similar to F2 hybrids. We scored eye sizes for 121 wild fish and correlated these measurements with their *cx50* genotypes. The T39M allele strongly correlated to eye size in this wild population ($p<0.0001$, Kruskal-Wallis test; Extended Data Fig. 2i), indicating a critical association of Cx50 with eye size reduction across distinct cavefish populations.

Eye degeneration confers a selective advantage in cave animals by reducing metabolic needs in a nutrient depleted environment (Moran et al., 2015). Our findings of two alleles of *cx50* in independent cavefish populations suggests that these *cx50* mutations affect metabolic success. To assess if there is an advantage for fish homozygous for the *cx50* cave allele, we measured 121 fish from the Calera cave for their condition factor (weight/length) (Extended Data Fig. 6b). 79 were homozygous for the cave allele, and 38 carried at least one surface allele. Overall, 53 (67.1%) fish homozygous for the cave allele had a higher proportional weight than the exponential regression of the fish carrying surface alleles, while 26 (32.9%) had a lower proportional weight (Extended Data Fig. 6c; p=0.0024, two-tailed Chi-square test). Exponential regressions suggest that fish homozygous for the cave allele have an average weight of about 5% heavier at a standard length of 4 cm, 10% at 5 cm, and 15% at 6 cm compared to homozygous reference surface fish. Moran et al. (2015) and these results strongly suggest a potential selective advantage of the mutated *cx50* alleles, supporting the hypotheses that eye reduction enhances survival and fitness in dark, resource-limited settings.

Variants in Cx50 across cavefishes and subterranean mammals

Given the independent mutations in Cx50 in two *Astyanax* cavefish lineages, we investigated the possibility that Cx50 could be involved in the reduced or absent eyes in other cave-adapted fish species. We evaluated publicly available sequences of 19 other cavefishes and their closest available surface relatives using the first 245 N-terminal amino acids which encompass the transmembrane domains (Extended Data Fig. 7, Supplementary Information 6). We found that there is 98% amino acid sequence homology in all examined surface fish species. Out of 19 cavefish species, eight of them showed non-synonymous SNPs in regions of *cx50* known to have phenotypic effects in humans, such as the N-terminal helix (NTH) and first two transmembrane domains (TM1, TM2, Extended Data Fig. 7).

Subterranean mammals, such as mole-rats, also have convergent eye degeneration (Fang et al., 2014; Partha et al., 2017; Springer et al., 2023). Teleost Cx50 and mammalian CX50 have an approximate 83% amino acid sequence similarity in the first 245 amino acids, demonstrating the high conservation of this protein across vertebrates. To evaluate CX50 as a possible example of molecular convergence in mammals, we compared *Cx50* sequences from five published genomes of subterranean-adapted mammals and their closest available surface relatives (Extended Data Fig. 8, Supplementary Information 6). Four of these mammals showed nonsynonymous SNPs in the NTH or first two transmembrane domains.

Due to extensive functional testing of human-cataract CX50 variants in the NTH, TM1, and TM2, we focused on mutations in these regions that are associated with subterranean-living (Fig. 3). To evaluate the potential effect of these mutations on protein function, we first conducted *in silico* analysis of Cx50/CX50 in seven cavefish species, three mammals, and their closest surface relatives. We used AlphaFold2 and comparison with the cryo-electron microscopy-resolved CX50 structure to predict the intracellular channel conformation of the N-terminal 245 residues of Cx50 or CX50 (Fig. 3b; Flores et al., 2020; Jumper et al., 2021; Myers et al., 2018), and then used ChimeraX to visualize static structural models of Cx50/CX50 gap junction formation (Pettersen et al., 2021).

These static models allow for the assessment of gross changes to the pore, such as the open-state conformation, orientation of functional elements like the N-terminal helix, and electrostatic potential (Extended Data Fig. 9a). In previous studies, these elements of the protein, especially in the inner pore regions of the NTH, TM1, and TM2, drastically alter the selectivity and conductance of the pore. Functional changes in CX50 pore result in cataracts, reduced proliferation, and increased apoptosis by interrupting antioxidant and growth factor distribution essential for lens survival (Liu et al., 2020; Tong et al., 2024; Yue et al., 2021).

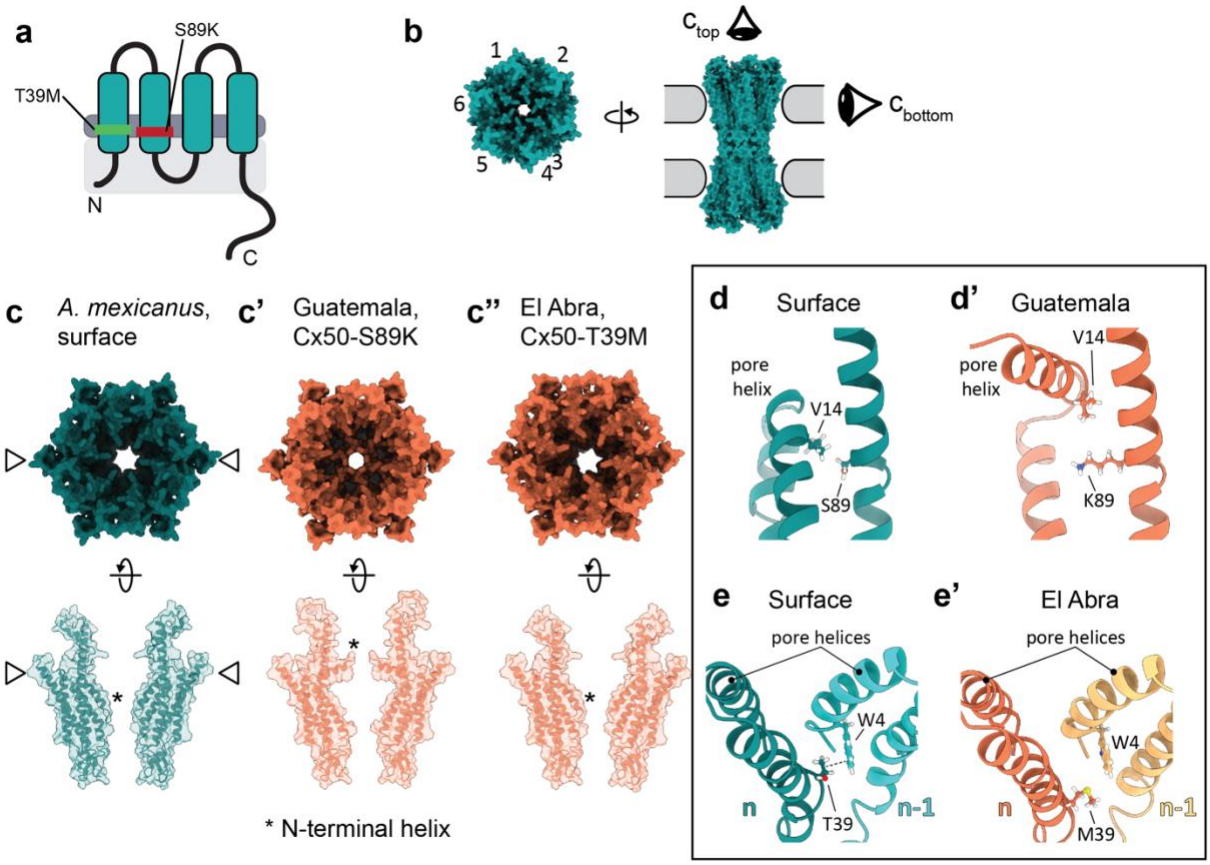

Figure 3. Predicted Cx50 structure in *Astyanax mexicanus*. (a) Connexin 50 is a transmembrane protein with four domains and a disorganized intercellular C-terminus. In *A. mexicanus* cave populations, T39M in El Abra lineage cavefish is in transmembrane 1 (TM1), S89K in Guatemala lineage cavefish is in transmembrane 2 (TM2). **(b)** CX50 modeling of gap junctions across the plasma membrane. Six CX50 proteins form a hemichannel in one cell membrane and couples with a hemichannel on an adjacent cell. The N-terminal helix (NTH) in the interior of the connexin pore contributes to ion selectivity and voltage gating and controls the stability of open and closed states by interacting with transmembranes 1 and 2. **(c-c'')** Modeling of the interior of the pore in *A. mexicanus* variants. Top figures are models visualized down the center of the pore. Bottom figures are cross sections of one side of the pore between subunits 6 and 3. Position of the NTH are indicated with an asterisk. Note that the Guatemala allele results in the N-terminus helix flipped up into the pore. **(d-e)** Molecular

renderings of the altered variants in cavefish and the key amino acids with which they interact. **(d)** Comparison of the interaction between aa89 in TM2 and the N-terminal helix of a single Cx50. In the surface protein, S89 and V14 pack closely together. **(d')** In the S89K variant of Guatemala lineage cavefish, lysine increases steric hinderance and alters the hydrophobic interaction with V14, pushing the NTH into the pore. **(g)** Comparison of the interaction between aa39 (n) and W4 in the N-terminal helix of an adjacent Connexin-50 protein (n-1). M39 reduces the stability of the NTH across the subunits and increased packing away from the pore.

We first modeled the *Astyanax* Cx50 variants found in our cave populations – S89K and T39M (Fig. 3c-e'). In the previously cryo-resolved structure of CX50, hydrophobic interactions between the NTH and TM2 are required for proper voltage gating and channel open stability (Jaradat et al., 2022). In our models of Cx50 with the Caballo Moro and Guatemala lineage S89K mutation, the NTH is repositioned into the channel opening due to increased steric hinderance of K89 and the hydrophobic side of the NTH (Fig. 3d-d', Extended Data Fig. 9). This results in a stabilized closed-state conformation and a smaller predicted interior pore that has the potential to disrupt channel function (Extended Data Fig. 9b). One of the other cavefish analyzed, the Chinese blind golden-line barbel, *Sinocyclocheilus anophthalmus*, has an S89F mutation at the same residue as the Guatemala lineage fish and a R33Q mutation at the same residue as a known human cataract phenotype (Extended Data Fig. 10a-d; Li et al., 2021; Villanelo et al., 2024). Similar to the Caballo Moro and Guatemala Cx50 proteins, the two mutations in *S. anophthalmus* can potentially reposition the NTH up into and narrow the pore (Extended Data Fig. 10a-c).

In contrast, the T39M mutation carried by El Abra fish leads to an enlarged predicted pore diameter (Fig. 3c"). In previously resolved and tested structures, T39 in TM1 on one subunit interacts with W4 in the NTH of an adjacent subunit to maintain a set distance between the domains (Fig. 3e-e'; Tong et al., 2021). M39 disrupts this interaction, which ultimately increases the predicted pore size in the most intracellular portion of the pore (Fig. 3c, e', Extended Data Fig. 9c). This phenotype is similar to the human T39R SNP which causes apoptosis and cataracts by stabilizing the open conformation and enhancing hemichannel function (Tong et al., 2021).

Of the subterranean mammals, CX50 from the Damara mole-rat, *Fukomys damarensis*, showed the most remarkable predicted structure change (Extended Data Fig. 10e-f). The Damara mole-rat has small eyes and heavy eyelids that impair vision (Bennett & Faulkes, 2000). There is a negatively charged glutamic acid change to a polar, uncharged glutamine in the intracellular N-terminal helix (E12Q). In some AlphaFold models we observed repositioning of the NTH into the pore and a narrowing of the pore diameter relative to a mouse structural model (Extended Data Fig. 10d-e'). In models where the NTH remained in the down conformation we would still expect a negative effect on pore properties. Residue E12 faces towards the interior of the pore, and we predict that the E12Q change would affect ion conductance, as CX50 has selectivity for cations that depends upon a number of negatively charged pore residues (Extended Data Fig. 10e-f; Jaradat et al., 2022).

These models suggest that Cx50/CX50 variants found in subterranean-dwelling creatures are an example of molecular convergence – with the same gene evolving mutations that affect protein function under similar environmental pressures. To assess the validity of our predicted protein effect pipeline, we selected the eyeless Caballo Moro Cx50-S89K variant to test for eye phenotypes *in vivo* (Fig. 4). We genetically engineered mice that recapitulated the S89K mutation at the endogenous locus. Mice homozygous for the CX50-S89K mutation developed congenital cataracts (Fig. 4b-c). They also showed smaller eyes ($p<0.0001$) and smaller lenses relative to homozygous wildtype siblings (Fig. 4; $p<0.0001$, Kruskal-Wallis test). Heterozygous siblings also exhibited reduced eye and lens sizes ($p<0.0001$ and $p=0.0006$, respectively, Kruskal-Wallis test), indicating a dominant effect of this allele that was also been reported for certain human SNPs (Arora et al., 2006; Banks et al., 2009; Jin et al., 2022; Shi et al., 2022). These *in vivo* results not only confirm the contribution of the GJA8-S89K mutation to eye size but also demonstrate the robustness of our protein modeling pipeline in identifying functionally significant convergent evolutionary changes.

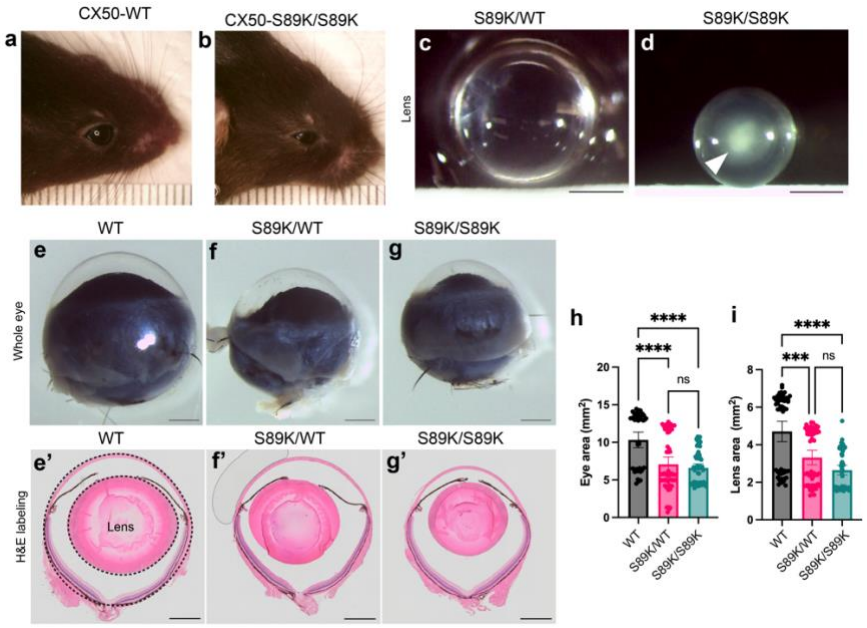

Figure 4. Testing SNPs with predicted CX50 protein function *in vivo*. (a-b) Differences in eye size between wild-type and homozygous CX50-S89K mice can be visualized externally. Ruler is in mm. **(c-d)** Imaging of dissected lens from adult heterozygous and homozygous CX50-S89K littermates (n=9). **(c)** Heterozygous lenses are transparent. **(d)** CX50-S89K mutants are opaque with a cataract (arrowhead). **(e-g')** Eye and lens visualization. Bar is 1cm. **(e-g)** Whole eye visualization of WT, heterozygous, and homozygous for the CX50-S89K allele in adult mice. **(e'-g')** H&E labeling of section of the eye for measurements of the eye and lens. Outlines indicate the diameter of the eye and lens. **(h-i)** Quantification of eye sections. Multiple sections were measured for each eye (mice n=11, sections n=170). **(h)** Quantification of eye area from H&E labels (**** $p<0.0001$, Kruskal-Wallis test, error bars are 95% confidence interval). **(i)** Quantification of lens area from H&E labeling (*** $p=0.0006$, **** $p<0.0001$, Kruskal-Wallis test, error bars are 95% confidence interval).

In this study, we demonstrated the power of a unique *A. mexicanus* cavefish population to identify the first protein-coding mutation contributing to eye degeneration. We find that mutations in Connexin50 play a pivotal role in eye degeneration across independent cavefish populations. Eye degeneration is a remarkable example of convergent evolution across many cave-inhabiting animals, suggesting an adaptive advantage to reducing the metabolic expense of eyes in completely dark environments. Further, our identified Cx50 mutations in other cavefish and subterranean mammals with predicted effects on gap junction functions. Due to its restricted expression almost exclusively in the lens, Connexin50 mutations are less likely to affect structures outside of the visual system, making it a prime candidate for strong evolutionary pressures. Our results underscore molecular convergence as a fundamental mechanism underpinning eye degeneration across taxa, offering profound insights into the adaptive landscapes of subterranean fauna.

Funding:
RK, SB, DA, and NR were supported by institutional funding from the Stowers Institute for Medical Research. Additionally, NR is supported by the Edward Mallinckrodt Foundation, NIH Grant R01 GM127872, DP2AG071466, and EDGE award 1923372. RK, SEM, and NR were additionally supported by NSF IOS-DEB 2316785. CPOG was supported by PAPIIT UNAM, IN214624. LE, EC, and JR were supported by Marist College.

Acknowledgements:
We thank M. Kirkman, J. Yonke, K. Zueckert-Gaudenz, and A. Kenzior for sample preparation and processing. We additionally thank J. Espinasa and students of the BIOL320 Genetics courses at Marist College for DNA sequencing and morphology measurements of Calera cavefish. We are grateful for N. Morris and M. Frangello for mouse care and lens imaging; the Stowers Aquatics facility for fish care and support; J. Hunter for eye quantifications; and J. VanCampen, G. Kong, and J.K. Medley for computational assistance.

Author contributions:
Conceptualization: LE, NR, RK, and SEM; Fieldwork: CPOG, LE, NR, EC, and JR; Cavefish phenotyping: LE and RK; Sequencing: KW and LE; Computational analysis: RK, CS, RLM, and DA; Cavefish CRISPants: SB and BT; Protein modeling: WBR and JU; Mouse phenotyping: YW; Writing and editing: RK, LE, NR, and SEM.

Data availability:
All sequencing data generated for this project is available under PRJNA841601, SRA accessions are listed in Supplementary Information 7. The surface fish *Astyanax mexicanus* reference genome (AstMex3_surface Accession # GCF_023375975.1) is available on NCBI.

Code availability:
Custom code for data processing and analysis is available on GitHub (https://github.com/rikellermeyer/Caballo_Moro).

Material availability:
Cryopreserved CX50-S89K mouse embryos are available on request.

Competing interests:
The authors declare no competing or financial interests.

Correspondence and requests for materials should be addressed to Riley Kellermeyer.

References

Aiello, L. C., & Wheeler, P. (1995). The Expensive-Tissue Hypothesis: The Brain and the Digestive System in Human and Primate Evolution. *Current Anthropology*, *36*(2), 199–221. https://doi.org/10.1086/204350

Alunni, A., Menuet, A., Candal, E., Pénigault, J.-B., Jeffery, W. R., & Rétaux, S. (2007). Developmental mechanisms for retinal degeneration in the blind cavefish Astyanax mexicanus. *Journal of Comparative Neurology*, *505*(2), 221–233. https://doi.org/10.1002/cne.21488

Arora, A., Minogue, P. J., Liu, X., Reddy, M. A., Ainsworth, J. R., Bhattacharya, S. S., Webster, A. R., Hunt, D. M., Ebihara, L., Moore, A. T., Beyer, E. C., & Berthoud, V. M. (2006). A novel GJA8 mutation is associated with autosomal dominant lamellar pulverulent cataract: Further evidence for gap junction dysfunction in human cataract. *Journal of Medical Genetics*, *43*(1), e2. https://doi.org/10.1136/jmg.2005.034108

Atukorala, A. D. S., & Franz-Odendaal, T. A. (2018). Genetic linkage between altered tooth and eye development in lens-ablated *Astyanax mexicanus*. *Developmental Biology*, *441*(2), 235–241. https://doi.org/10.1016/j.ydbio.2018.07.008

Banks, E. A., Toloue, M. M., Shi, Q., Zhou, Z. J., Liu, J., Nicholson, B. J., & Jiang, J. X. (2009). Connexin mutation that causes dominant congenital cataracts inhibits gap junctions, but not hemichannels, in a dominant negative manner. *Journal of Cell Science*, *122*(3), 378–388. https://doi.org/10.1242/jcs.034124

Bennett, N. C., & Faulkes, C. G. (2000). *African Mole-Rats: Ecology and Eusociality*. Cambridge University Press.

Berry, V., Ionides, A., Pontikos, N., Moghul, I., Moore, A. T., Quinlan, R. A., & Michaelides, M. (2020). Whole Exome Sequencing Reveals Novel and Recurrent Disease-Causing Variants in Lens Specific Gap Junctional Protein Encoding Genes Causing Congenital Cataract. *Genes*, *11*(5), 512. https://doi.org/10.3390/genes11050512

Berthoud, V. M., & Ngezahayo, A. (2017). Focus on lens connexins. *BMC Cell Biology*, *18*(1), 6. https://doi.org/10.1186/s12860-016-0116-6

Borowsky, R., & Wilkens, H. (2002). Mapping a Cave Fish Genome: Polygenic Systems and Regressive Evolution. *Journal of Heredity*, *93*(1), 19–21. https://doi.org/10.1093/jhered/93.1.19

Bradic, M., Beerli, P., García-de León, F. J., Esquivel-Bobadilla, S., & Borowsky, R. L. (2012). Gene flow and population structure in the Mexican blind cavefish complex (Astyanax mexicanus). *BMC Evolutionary Biology*, *12*(1), 9. https://doi.org/10.1186/1471-2148-12-9

Ceroni, F., Aguilera-Garcia, D., Chassaing, N., Bax, D. A., Blanco-Kelly, F., Ramos, P., Tarilonte, M., Villaverde, C., da Silva, L. R. J., Ballesta-Martínez, M. J., Sanchez-Soler, M. J., Holt, R. J., Cooper-Charles, L., Bruty, J., Wallis, Y., McMullan, D., Hoffman, J., Bunyan, D., Stewart, A., … DDD Study. (2019). New GJA8 variants and phenotypes highlight its critical role in a broad spectrum of eye anomalies. *Human Genetics*, *138*(8), 1027–1042. https://doi.org/10.1007/s00439-018-1875-2

Dollo, L. (1893). THE LAWS OF EVOLUTION. *Bull. Soc. Geol. Pal. Hydro.*, *7:164-166*.

Dollo, L. (1922). Les Céphalopodes Déroulés et L'Irréversibilité de L'Évolution. *Bijdragen Tot de Dierkunde*. https://doi.org/10.1163/26660644-02201030

Elipot, Y., Hinaux, H., Callebert, J., & Rétaux, S. (2013). Evolutionary Shift from Fighting to Foraging in Blind Cavefish through Changes in the Serotonin Network. *Current Biology*, *23*(1), 1–10. https://doi.org/10.1016/j.cub.2012.10.044

Espinasa, L., & Borowsky, R. (2000). EYED CAVE FISH IN A KARST WINDOW. *Journal of Cave and Karst Studies*, *62*(3), 180–183.

Espinasa, L., Heintz, C., Rétaux, S., Yoshisawa, M., Agnès, F., Ornelas-Garcia, P., & Balogh-Robinson, R. (2021). Vibration attraction response is a plastic trait in blind Mexican tetra (), variable within subpopulations inhabiting the same cave. *Journal of Fish Biology*, *98*(1), 304–316. https://doi.org/10.1111/jfb.14586

Espinasa, L., Legendre, L., Fumey, J., Blin, M., Rétaux, S., & Espinasa, M. (2018). A new cave locality for Astyanax cavefish in Sierra de El Abra, Mexico. *Subterranean Biology*, *26*, 39–53. https://doi.org/10.3897/subtbiol.26.26643

Espinasa, L., Ornelas-García, C. P., Legendre, L., Rétaux, S., Best, A., Gamboa-Miranda, R., Espinosa-Pérez, H., & Sprouse, P. (2020). Discovery of Two New Astyanax Cavefish Localities Leads to Further Understanding of the Species Biogeography. *Diversity*, *12*(10), Article 10. https://doi.org/10.3390/d12100368

Fang, X., Seim, I., Huang, Z., Gerashchenko, M. V., Xiong, Z., Turanov, A. A., Zhu, Y., Lobanov, A. V., Fan, D., Yim, S. H., Yao, X., Ma, S., Yang, L., Lee, S.-G., Kim, E. B., Bronson, R. T., Šumbera, R., Buffenstein, R., Zhou, X., … Gladyshev, V. N. (2014). Adaptations to a Subterranean Environment and Longevity Revealed by the Analysis of Mole Rat Genomes. *Cell Reports*, *8*(5), 1354–1364. https://doi.org/10.1016/j.celrep.2014.07.030

590 Flores, J. A., Haddad, B. G., Dolan, K. A., Myers, J. B., Yoshioka, C. C., Copperman, J., Zuckerman,
591 D. M., & Reichow, S. L. (2020). Connexin-46/50 in a dynamic lipid environment resolved
592 by CryoEM at 1.9 Å. *Nature Communications*, *11*(1), 4331.
593 https://doi.org/10.1038/s41467-020-18120-5
594 Garduño-Sánchez, M., Hernández-Lozano, J., Moran, R. L., Miranda-Gamboa, R., Gross, J. B.,
595 Rohner, N., Elliott, W. R., Miller, J., Lozano-Vilano, L., McGaugh, S. E., & Ornelas-García, C.
596 P. (2023). Phylogeographic relationships and morphological evolution between cave and
597 surface Astyanax mexicanus populations (De Filippi 1853) (Actinopterygii, Characidae).
598 *Molecular Ecology*, *32*(20), 5626–5644. https://doi.org/10.1111/mec.17128
599 Ge, X.-L., Zhang, Y., Wu, Y., Lv, J., Zhang, W., Jin, Z.-B., Qu, J., & Gu, F. (2014). Identification of a
600 Novel GJA8 (Cx50) Point Mutation Causes Human Dominant Congenital Cataracts.
601 *Scientific Reports*, *4*(1), Article 1. https://doi.org/10.1038/srep04121
602 Gore, A. V., Tomins, K. A., Iben, J., Ma, L., Castranova, D., Davis, A. E., Parkhurst, A., Jeffery, W. R.,
603 & Weinstein, B. M. (2018). An epigenetic mechanism for cavefish eye degeneration.
604 *Nature Ecology & Evolution*, *2*(7), 1155–1160. https://doi.org/10.1038/s41559-018-
605 0569-4
606 Gross, J. B. (2012). The complex origin of Astyanax cavefish. *BMC Evolutionary Biology*, *12*, 105.
607 https://doi.org/10.1186/1471-2148-12-105
608 Hüppop, K. (1986). Oxygen consumption of Astyanax fasciatus (Characidae, Pisces): A
609 comparison of epigean and hypogean populations. *Environmental Biology of Fishes*,
610 *17*(4), 299–308. https://doi.org/10.1007/BF00001496

Huppop, K., & Wilkens, H. (1991). Bigger eggs in subterranean Astyanax fasciatus (Characidae, Pisces). *Journal of Zoological Systematics and Evolutionary Research*, *29*(4), 280–288. https://doi.org/10.1111/j.1439-0469.1991.tb00673.x

Jaradat, R., Li, X., Chen, H., Stathopulos, P. B., & Bai, D. (2022). The Hydrophobic Residues in Amino Terminal Domains of Cx46 and Cx50 Are Important for Their Gap Junction Channel Ion Permeation and Gating. *International Journal of Molecular Sciences*, *23*(19), Article 19. https://doi.org/10.3390/ijms231911605

Jeffery, W. R., & Martasian, D. P. (1998). Evolution of Eye Regression in the Cavefish Astyanax: Apoptosis and the Pax-6 Gene1. *American Zoologist*, *38*(4), 685–696. https://doi.org/10.1093/icb/38.4.685

Jin, A., Zhao, Q., Liu, S., Jin, Z., Li, S., Xiang, M., Zeng, M., & Jin, K. (2022). Identification of a New Mutation p.P88L in Connexin 50 Associated with Dominant Congenital Cataract. *Frontiers in Cell and Developmental Biology*, *10*, 794837. https://doi.org/10.3389/fcell.2022.794837

Jumper, J., Evans, R., Pritzel, A., Green, T., Figurnov, M., Ronneberger, O., Tunyasuvunakool, K., Bates, R., Žídek, A., Potapenko, A., Bridgland, A., Meyer, C., Kohl, S. A. A., Ballard, A. J., Cowie, A., Romera-Paredes, B., Nikolov, S., Jain, R., Adler, J., … Hassabis, D. (2021). Highly accurate protein structure prediction with AlphaFold. *Nature*, *596*(7873), 583–589. https://doi.org/10.1038/s41586-021-03819-2

Krishnan, J., & Rohner, N. (2017). Cavefish and the basis for eye loss. *Philosophical Transactions of the Royal Society B: Biological Sciences*, *372*(1713), 20150487. https://doi.org/10.1098/rstb.2015.0487

633 Lacey, E. A. (2000). *Life Underground: The Biology of Subterranean Rodents*. University of
634 Chicago Press.
635 Li, L., Fan, D.-B., Zhao, Y.-T., Li, Y., Yang, Z.-B., & Zheng, G.-Y. (2019). GJA8 missense mutation
636 disrupts hemichannels and induces cell apoptosis in human lens epithelial cells. *Scientific*
637 *Reports*, *9*(1), Article 1. https://doi.org/10.1038/s41598-019-55549-1
638 Li, R., Wang, X., Bian, C., Gao, Z., Zhang, Y., Jiang, W., Wang, M., You, X., Cheng, L., Pan, X., Yang,
639 J., & Shi, Q. (2021). Whole-Genome Sequencing of Sinocyclocheilus maitianheensis
640 Reveals Phylogenetic Evolution and Immunological Variances in Various Sinocyclocheilus
641 Fishes. *Frontiers in Genetics*, *12*.
642 https://www.frontiersin.org/article/10.3389/fgene.2021.736500
643 Liu, J., Riquelme, M. A., Li, Z., Li, Y., Tong, Y., Quan, Y., Pei, C., Gu, S., & Jiang, J. X. (2020).
644 Mechanosensitive collaboration between integrins and connexins allows nutrient and
645 antioxidant transport into the lens. *Journal of Cell Biology*, *219*(12), e202002154.
646 https://doi.org/10.1083/jcb.202002154
647 Lyon, A., Powers, A. K., Gross, J. B., & O'Quin, K. E. (2017). Two – three loci control scleral ossicle
648 formation via epistasis in the cavefish Astyanax mexicanus. *PLOS ONE*, *12*(2), e0171061.
649 https://doi.org/10.1371/journal.pone.0171061
650 Ma, L., Gore, A. V., Castranova, D., Shi, J., Ng, M., Tomins, K. A., van der Weele, C. M., Weinstein,
651 B. M., & Jeffery, W. R. (2020). A hypomorphic cystathionine ß-synthase gene contributes
652 to cavefish eye loss by disrupting optic vasculature. *Nature Communications*, *11*(1),
653 Article 1. https://doi.org/10.1038/s41467-020-16497-x

McGaugh, S. E., Gross, J. B., Aken, B., Blin, M., Borowsky, R., Chalopin, D., Hinaux, H., Jeffery, W. R., Keene, A., Ma, L., Minx, P., Murphy, D., O'Quin, K. E., Rétaux, S., Rohner, N., Searle, S. M. J., Stahl, B. A., Tabin, C., Volff, J.-N., … Warren, W. C. (2014). The cavefish genome reveals candidate genes for eye loss. *Nature Communications*, *5*(1), Article 1. https://doi.org/10.1038/ncomms6307

Minogue, P. J., Tong, J.-J., Arora, A., Russell-Eggitt, I., Hunt, D. M., Moore, A. T., Ebihara, L., Beyer, E. C., & Berthoud, V. M. (2009). A Mutant Connexin50 with Enhanced Hemichannel Function Leads to Cell Death. *Investigative Ophthalmology & Visual Science*, *50*(12), 5837–5845. https://doi.org/10.1167/iovs.09-3759

Miranda-Gamboa, R., Espinasa, L., Verde-Ramírez, M. de los A., Hernández-Lozano, J., Lacaille, J. L., Espinasa, M., & Ornelas-García, C. P. (2023). A new cave population of Astyanax mexicanus from Northern Sierra de El Abra, Tamaulipas, Mexico. *Subterranean Biology*, *45*, 95–117. https://doi.org/10.3897/subtbiol.45.98434

Mitchell, R. W., Russell, W. H., & Elliott, W. R. (1977). Mexican Eyeless Characin Fishes, Genus Astyanax: Environment, Distribution, and Evolution. *Special Publications the Museum Texas Tech University*.

Moran, D., Softley, R., & Warrant, E. J. (2015). The energetic cost of vision and the evolution of eyeless Mexican cavefish. *Science Advances*, *1*(8), e1500363. https://doi.org/10.1126/sciadv.1500363

Moran, R. L., Richards, E. J., Ornelas-García, C. P., Gross, J. B., Donny, A., Wiese, J., Keene, A. C., Kowalko, J. E., Rohner, N., & McGaugh, S. E. (2023). Selection-driven trait loss in

independently evolved cavefish populations. *Nature Communications*, *14*(1), 2557. https://doi.org/10.1038/s41467-023-37909-8

Myers, J. B., Haddad, B. G., O'Neill, S. E., Chorev, D. S., Yoshioka, C. C., Robinson, C. V., Zuckerman, D. M., & Reichow, S. L. (2018). Structure of native lens connexin 46/50 intercellular channels by cryo-EM. *Nature*, *564*(7736), Article 7736. https://doi.org/10.1038/s41586-018-0786-7

Niemiller, M. L., Fitzpatrick, B. M., Shah, P., Schmitz, L., & Near, T. J. (2013). Evidence for Repeated Loss of Selective Constraint in Rhodopsin of Amblyopsid Cavefishes (TELeostei: Amblyopsidae). *Evolution*, *67*(3), 732–748. https://doi.org/10.1111/j.1558-5646.2012.01822.x

O'Quin, K. E., Yoshizawa, M., Doshi, P., & Jeffery, W. R. (2013). Quantitative Genetic Analysis of Retinal Degeneration in the Blind Cavefish Astyanax mexicanus. *PLoS ONE*, *8*(2), e57281. https://doi.org/10.1371/journal.pone.0057281

Pal, J. D., Berthoud, V. M., Beyer, E. C., Mackay, D., Shiels, A., & Ebihara, L. (1999). Molecular mechanism underlying a Cx50-linked congenital cataract. *American Journal of Physiology-Cell Physiology*, *276*(6), C1443–C1446. https://doi.org/10.1152/ajpcell.1999.276.6.C1443

Partha, R., Chauhan, B. K., Ferreira, Z., Robinson, J. D., Lathrop, K., Nischal, K. K., Chikina, M., & Clark, N. L. (2017). Subterranean mammals show convergent regression in ocular genes and enhancers, along with adaptation to tunneling. *eLife*, *6*, e25884. https://doi.org/10.7554/eLife.25884

Pettersen, E. F., Goddard, T. D., Huang, C. C., Meng, E. C., Couch, G. S., Croll, T. I., Morris, J. H., & Ferrin, T. E. (2021). UCSF ChimeraX: Structure visualization for researchers, educators, and developers. *Protein Science: A Publication of the Protein Society*, *30*(1), 70–82. https://doi.org/10.1002/pro.3943

Ping, X., Liang, J., Shi, K., Bao, J., Wu, J., Yu, X., Tang, X., Zou, J., & Shentu, X. (2021). Rapamycin relieves the cataract caused by ablation of Gja8b through stimulating autophagy in zebrafish. *Autophagy*, *17*(11), 3323–3337. https://doi.org/10.1080/15548627.2021.1872188

Policarpo, M., Legendre, L., Germon, I., Lafargeas, P., Espinasa, L., Rétaux, S., & Casane, D. (2024). The nature and distribution of putative non-functional alleles suggest only two independent events at the origins of Astyanax mexicanus cavefish populations. *BMC Ecology and Evolution*, *24*(1), 41. https://doi.org/10.1186/s12862-024-02226-1

Protas, M., Conrad, M., Gross, J. B., Tabin, C., & Borowsky, R. (2007). Regressive Evolution in the Mexican Cave Tetra, Astyanax mexicanus. *Current Biology*, *17*(5), 452–454. https://doi.org/10.1016/j.cub.2007.01.051

Protas, M., Tabansky, I., Conrad, M., Gross, J. B., Vidal, O., Tabin, C. J., & Borowsky, R. (2008). Multi-trait evolution in a cave fish, Astyanax mexicanus. *Evolution & Development*, *10*(2), 196–209. https://doi.org/10.1111/j.1525-142X.2008.00227.x

Shi, Y., Li, X., & Yang, J. (2022). Mutations of CX46/CX50 and Cataract Development. *Frontiers in Molecular Biosciences*, *9*. https://doi.org/10.3389/fmolb.2022.842399

Shiels, A., Mackay, D., Ionides, A., Berry, V., Moore, A., & Bhattacharya, S. (1998). A missense mutation in the human connexin50 gene (GJA8) underlies autosomal dominant “zonular

pulverulent" cataract, on chromosome 1q. *American Journal of Human Genetics*, *62*(3), 526–532.

Soares, D., Yamamoto, Y., Strickler, A. G., & Jeffery, W. R. (2004). The Lens Has a Specific Influence on Optic Nerve and Tectum Development in the Blind Cavefish Astyanax. *Developmental Neuroscience*, *26*(5–6), 308–317. https://doi.org/10.1159/000082272

Springer, M. S., Emerling, C. A., & Gatesy, J. (2023). Three Blind Moles: Molecular Evolutionary Insights on the Tempo and Mode of Convergent Eye Degeneration in Notoryctes typhlops (Southern Marsupial Mole) and Two Chrysochlorids (Golden Moles). *Genes*, *14*(11), Article 11. https://doi.org/10.3390/genes14112018

Stahl, B. A., Peuß, R., McDole, B., Kenzior, A., Jaggard, J. B., Gaudenz, K., Krishnan, J., McGaugh, S. E., Duboue, E. R., Keene, A. C., & Rohner, N. (2019). Stable transgenesis in Astyanax mexicanus using the Tol2 transposase system. *Developmental Dynamics : An Official Publication of the American Association of Anatomists*, *248*(8), 679–687. https://doi.org/10.1002/dvdy.32

Sun, W., Xiao, X., Li, S., Guo, X., & Zhang, Q. (2011). Mutational screening of six genes in Chinese patients with congenital cataract and microcornea. *Molecular Vision*, *17*, 1508–1513.

Tong, J.-J., Khan, U., Haddad, B. G., Minogue, P. J., Beyer, E. C., Berthoud, V. M., Reichow, S. L., & Ebihara, L. (2021). Molecular mechanisms underlying enhanced hemichannel function of a cataract-associated Cx50 mutant. *Biophysical Journal*, *120*(24), 5644–5656. https://doi.org/10.1016/j.bpj.2021.11.004

Tong, Y., Wang, G., Riquelme, M. A., Du, Y., Quan, Y., Fu, J., Gu, S., & Jiang, J. X. (2024). Mechano-activated connexin hemichannels and glutathione transport protect lens fiber cells

740 against oxidative insults. *Redox Biology*, *73*, 103216.
741 https://doi.org/10.1016/j.redox.2024.103216
742 Vanita, V., Singh, J. R., Singh, D., Varon, R., & Sperling, K. (2008). A mutation in GJA8 (p.P88Q) is
743 associated with “balloon-like” cataract with Y-sutural opacities in a family of Indian
744 origin. *Molecular Vision*, *14*, 1171–1175.
745 Villanelo, F., Minogue, P. J., Maripillán, J., Reyna-Jeldes, M., Jensen-Flores, J., García, I. E., Beyer,
746 E. C., Pérez-Acle, T., Berthoud, V. M., & Martínez, A. D. (2024). Connexin channels and
747 hemichannels are modulated differently by charge reversal at residues forming the
748 intracellular pocket. *Biological Research*, *57*(1), 31. https://doi.org/10.1186/s40659-024-
749 00501-5
750 Warren, W. C., Boggs, T. E., Borowsky, R., Carlson, B. M., Ferrufino, E., Gross, J. B., Hillier, L., Hu,
751 Z., Keene, A. C., Kenzior, A., Kowalko, J. E., Tomlinson, C., Kremitzki, M., Lemieux, M. E.,
752 Graves-Lindsay, T., McGaugh, S. E., Miller, J. T., Mommersteeg, M. T. M., Moran, R. L., …
753 Rohner, N. (2021). A chromosome-level genome of Astyanax mexicanus surface fish for
754 comparing population-specific genetic differences contributing to trait evolution. *Nature*
755 *Communications*, *12*(1), 1447. https://doi.org/10.1038/s41467-021-21733-z
756 White, T. W., Goodenough, D. A., & Paul, D. L. (1998). Targeted Ablation of Connexin50 in Mice
757 Results in Microphthalmia and Zonular Pulverulent Cataracts. *Journal of Cell Biology*,
758 *143*(3), 815–825. https://doi.org/10.1083/jcb.143.3.815
759 Wiese, J., Richards, E., Kowalko, J. E., & McGaugh, S. E. (2024). Quantitative trait loci
760 concentrate in specific regions of the Mexican cavefish genome and reveal key candidate

genes for cave-associated evolution. *Journal of Heredity*, esae040. https://doi.org/10.1093/jhered/esae040

Yamamoto, Y., & Jeffery, W. R. (2000). Central Role for the Lens in Cave Fish Eye Degeneration. *Science*, *289*(5479), 631–633. https://doi.org/10.1126/science.289.5479.631

Yamamoto, Y., Stock, D. W., & Jeffery, W. R. (2004). Hedgehog signalling controls eye degeneration in blind cavefish. *Nature*, *431*(7010), 844–847. https://doi.org/10.1038/nature02864

Yoshizawa, M., Gorički, Š., Soares, D., & Jeffery, W. R. (2010). Evolution of a Behavioral Shift Mediated by Superficial Neuromasts Helps Cavefish Find Food in Darkness. *Current Biology*, *20*(18), 1631–1636. https://doi.org/10.1016/j.cub.2010.07.017

Yue, B., Haddad, B. G., Khan, U., Chen, H., Atalla, M., Zhang, Z., Zuckerman, D. M., Reichow, S. L., & Bai, D. (2021). Connexin 46 and connexin 50 gap junction channel properties are shaped by structural and dynamic features of their N-terminal domains. *The Journal of Physiology*, *599*(13), 3313–3335. https://doi.org/10.1113/JP281339

Zhao, Z., & Shen, Y. (2022). Rain-induced weathering dissolution of limestone and implications for the soil sinking-rock outcrops emergence mechanism at the karst surface: A case study in southwestern China. *Carbonates and Evaporites*, *37*(4), 69. https://doi.org/10.1007/s13146-022-00813-1